

## Lecture 11

### Surface Characterization of Biomaterials in Vacuum

The structure and chemistry of a biomaterial surface greatly dictates the degree of biocompatibility of an implant. Surface characterization is thus a central aspect of biomaterials research.

Surface chemistry can be investigated directly using high vacuum methods:

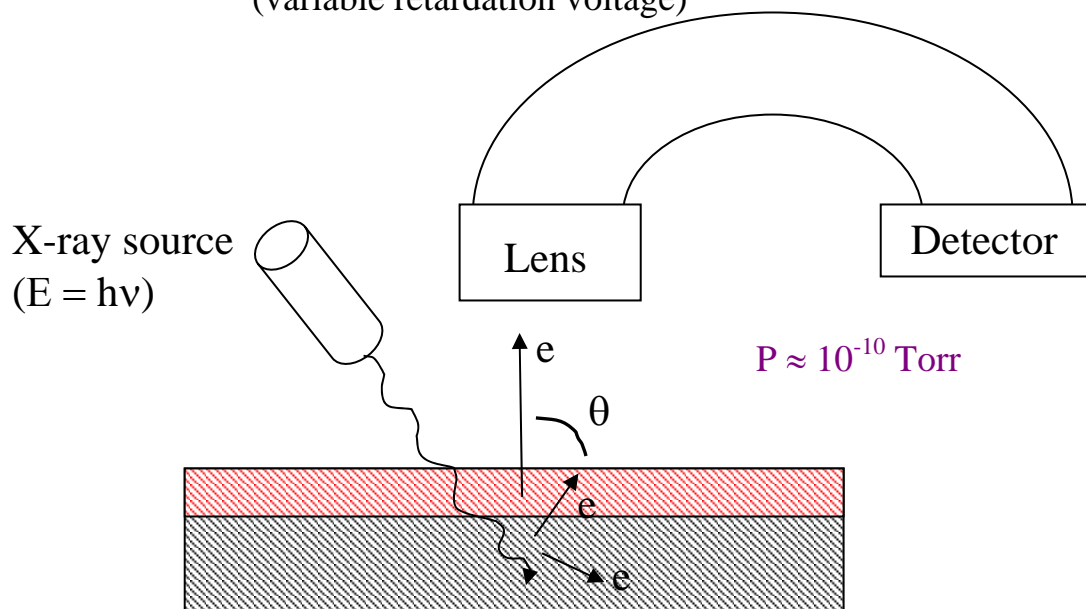
- Electron spectroscopy for Chemical Analysis (ESCA)/X-ray Photoelectron Spectroscopy (XPS)
- Auger Electron Spectroscopy (AES)
- Secondary Ion Mass Spectroscopy (SIMS)

#### 1. XPS/ESCA

##### Theoretical Basis:

- Secondary electrons ejected by x-ray bombardment from the sample near surface (0.5-10 nm) with characteristic energies
- Analysis of the photoelectron energies yields a quantitative measure of the surface composition

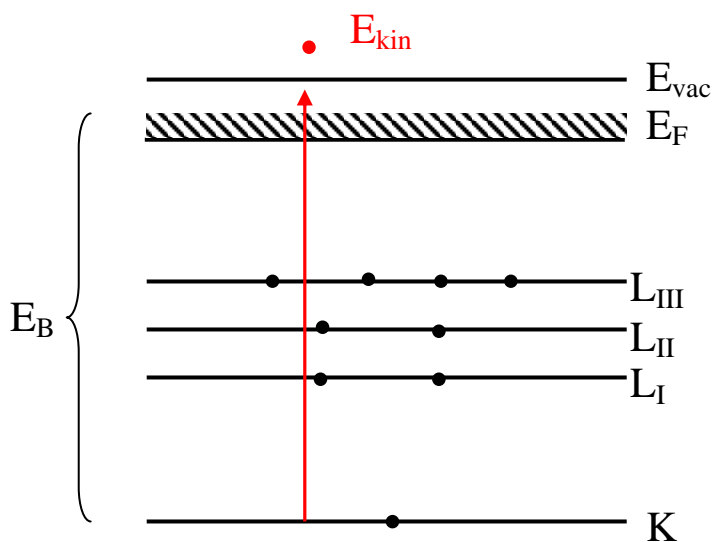
Electron energy analyzer  
(variable retardation voltage)



Photoelectron binding energy is characteristic of the **element** and **bonding environment**



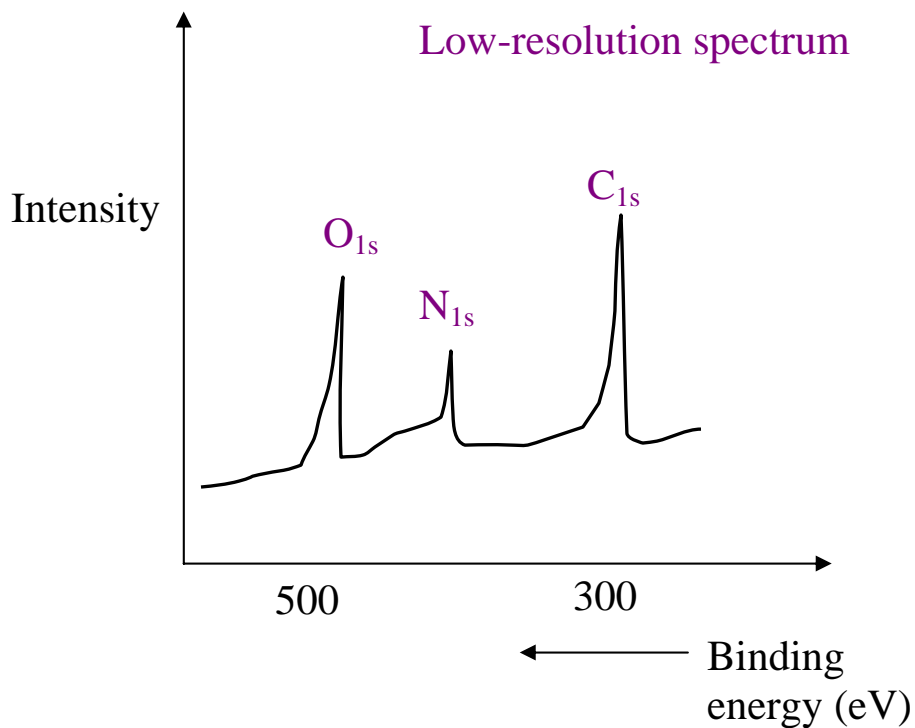
**Chemical analysis!**



Binding energy = incident x-ray energy – photoelectron kinetic energy

$$E_B = h\nu - E_{kin}$$

## Quantitative Elemental Analysis



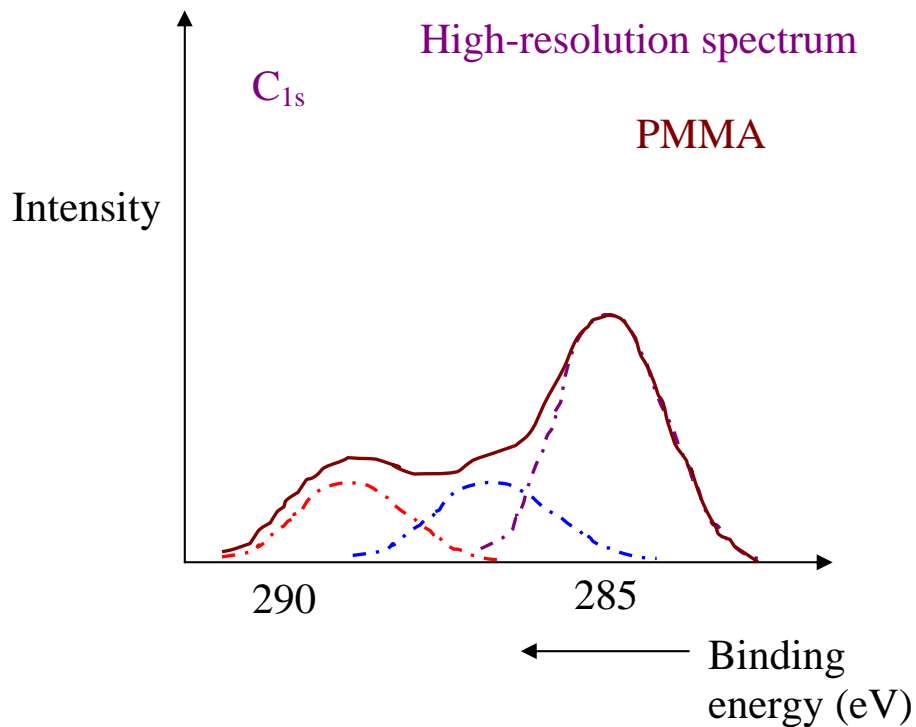
- Area under peak  $I_i \propto$  number of electrons ejected (& atoms present)
- Only electrons in the near surface region escape without losing energy by inelastic collision
- Sensitivity: depends on element. Elements present in concentrations  $>0.1$  atom% are generally detectable (H & He undetected)
- Quantification of atomic fraction  $C_i$  (of elements detected)

$$C_i = \frac{I_i / S_i}{\sum_j I_j / S_j}$$

sum over detected elements

$S_i$  is the *sensitivity factor*:

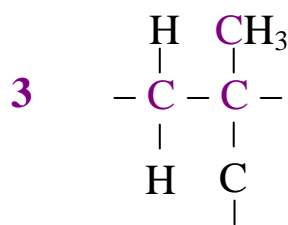
- $f(\text{instrument \& atomic parameters})$
- can be calculated



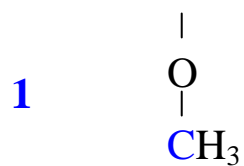
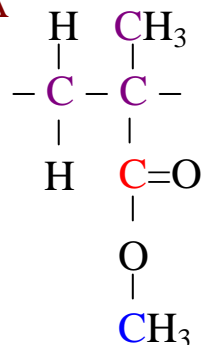
➤ Ratio of peak areas gives a ratio of photoelectrons ejected from atoms in a particular bonding configuration ( $S_i = \text{constant}$ )

5 carbons in total

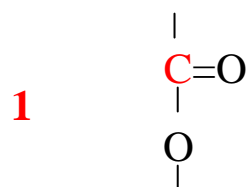
Ex. PMMA



(a) **Lowest  $E_B$   $C_{1s}$**   
 $E_B \approx 285.0 \text{ eV}$

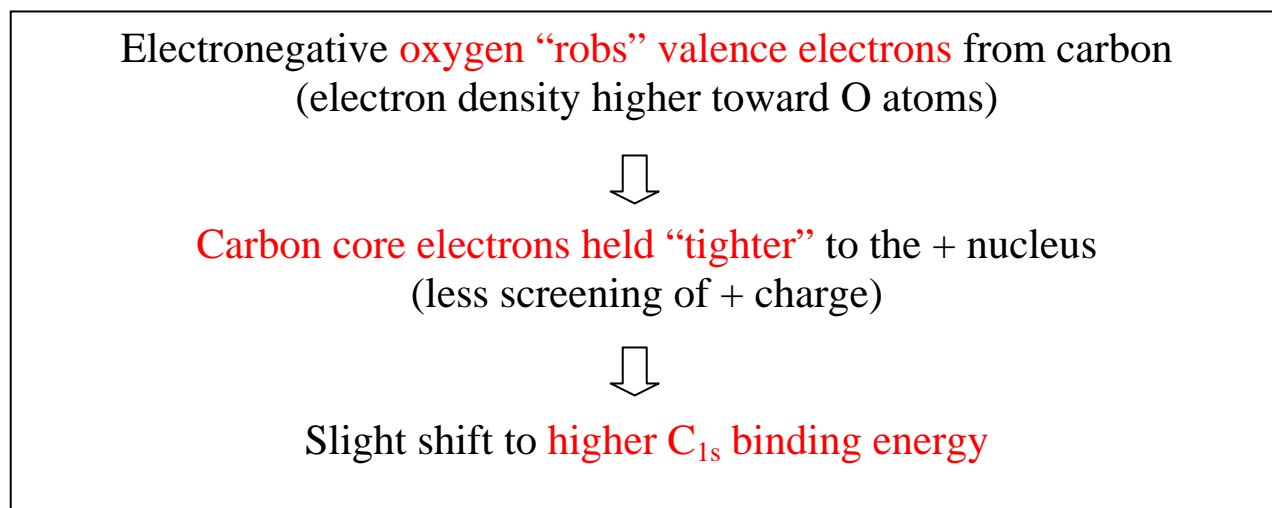


(b) **Intermediate  $E_B$   $C_{1s}$**   
 $E_B \approx 286.8 \text{ eV}$



(c) **Highest  $E_B$   $C_{1s}$**   
 $E_B \approx 289.0 \text{ eV}$

Why does *core* electron  $E_B$  vary with *valence* shell configuration?

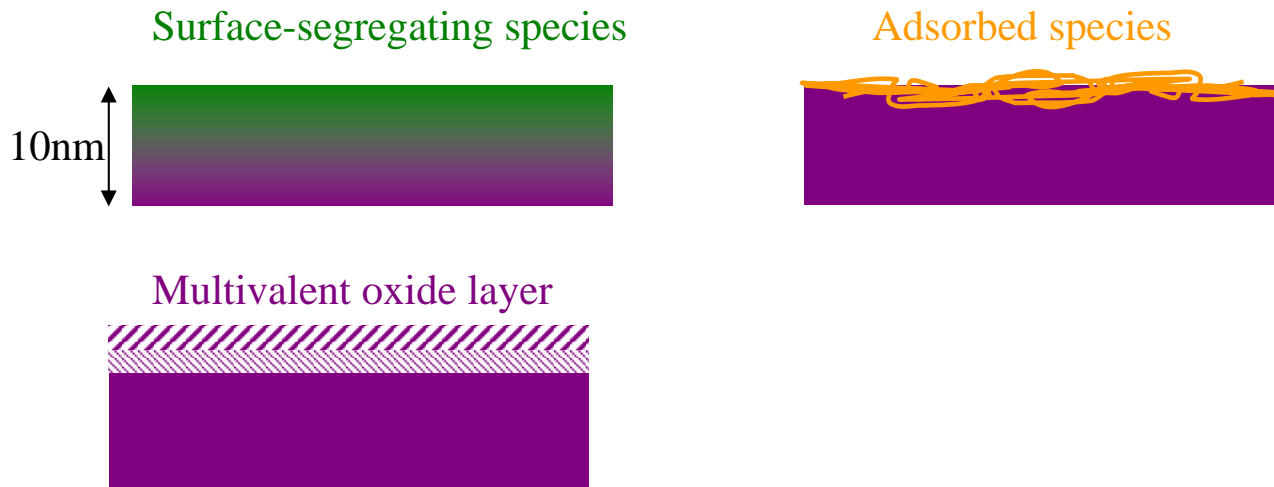


Similarly, different oxidation states of metals can be distinguished.



XPS signal comes from first ~10 nm of sample surface.

What if the sample has a concentration gradient within this depth?



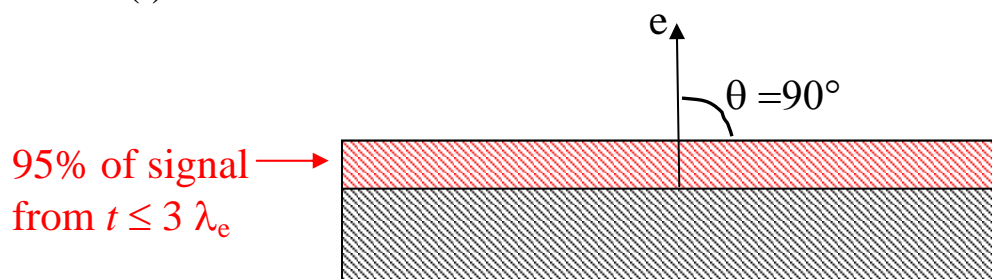
## Depth-Resolved ESCA/XPS

- The probability of a photoelectron escaping the sample without undergoing inelastic collision is inversely related to its depth  $t$  within the sample:

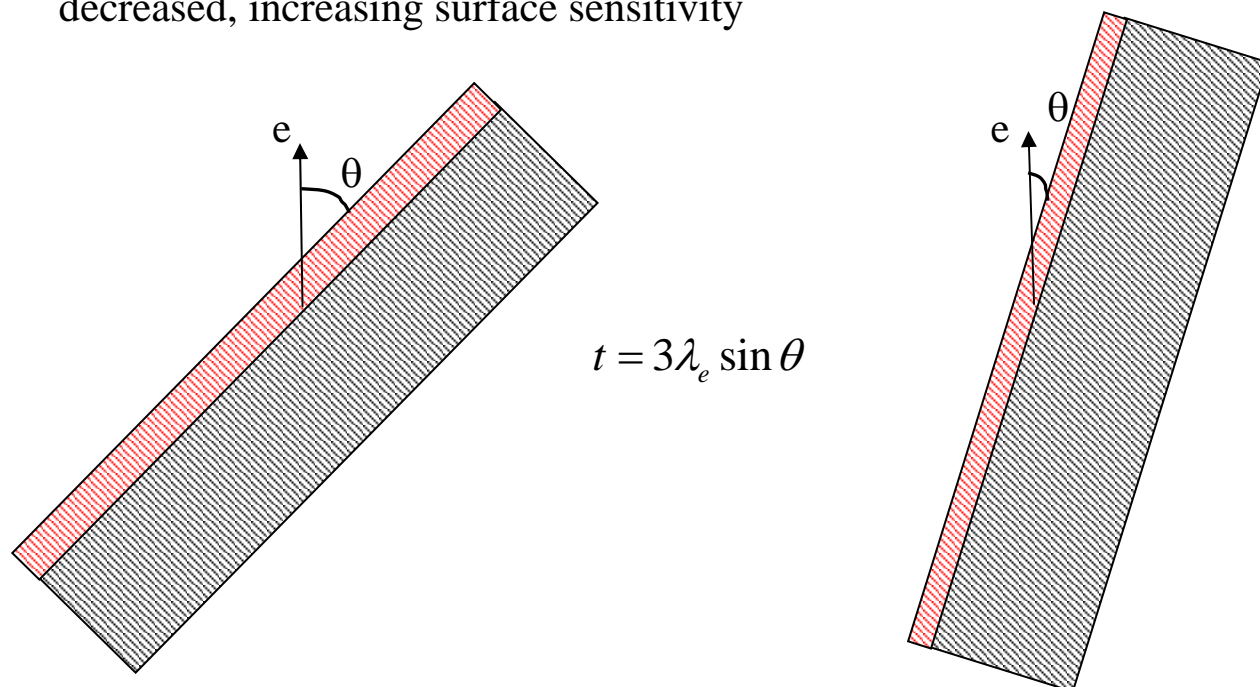
$$P(t) \sim \exp\left(\frac{-t}{\lambda_e}\right)$$

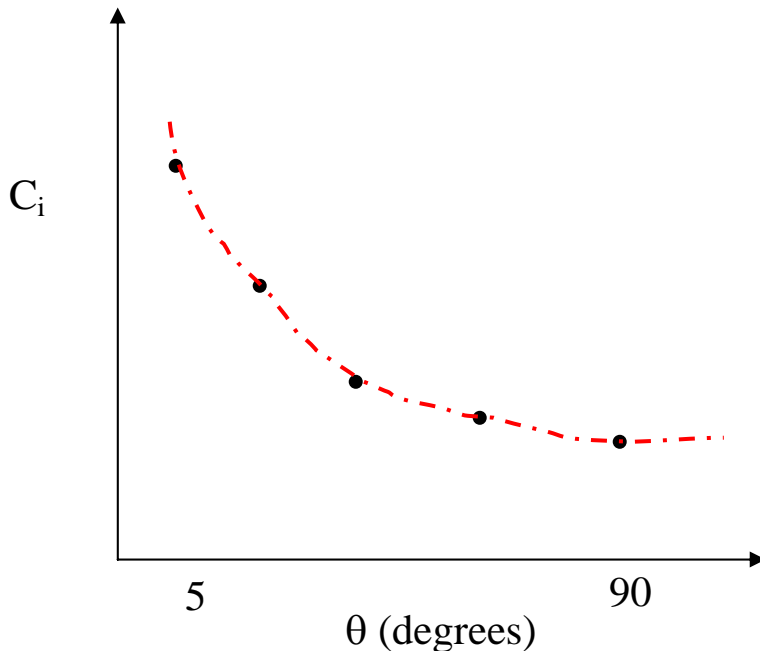
where  $\lambda_e$  (typically  $\sim 5\text{-}30 \text{ \AA}$ ) is the **electron inelastic mean-free path**, which depends on the electron kinetic energy and the material. (Physically,  $\lambda_e = \text{avg. distance traveled between inelastic collisions.}$ )

For  $t = 3 \lambda_e \Rightarrow P(t) = 0.05$



- By varying the **take-off angle** ( $\theta$ ), the sampling depth can be decreased, increasing surface sensitivity





➤ Variation of composition with angle may indicate:

- Preferential orientation at surface
- Surface segregation
- Adsorbed species (e.g., hydrocarbons)
- etc.

➤ Quantifying composition as a function of depth

The area under the  $j$ th peak of element  $i$  is the integral of attenuated contributions from all sample depths  $z$ :

$$I_{ij} = C_{inst} T(E_{kin}) L_{ij} \sigma_{ij} \int n_i(z) \exp\left(\frac{-z}{\lambda_e \sin \theta}\right) dz$$

$C_{inst}$  = instrument constant

$T(E_{kin})$  = analyzer transmission function

$L_{ij}$  = angular asymmetry factor for orbital  $j$  of element  $i$

$\sigma_{ij}$  is the photoionization cross-section

$n_i(z)$  is the atomic concn. of  $i$  at a depth  $z$  (atoms/vol)

For a semi-infinite sample of homogeneous composition:

$$I_{ij} = -I_{ij,o} n_i \lambda_e \sin \theta \exp\left(\frac{-z}{\lambda_e \sin \theta}\right) \Bigg|_0^\infty = I_{ij,o} n_i \lambda_e \sin \theta = S_i n_i = I_{ij,\infty}$$

where  $I_{ij,o} = C_{inst} T(E_{kin}) L_{ij} \sigma_{ij}$

Relative concentrations of elements (or atoms with a particular bond configuration) are obtained from ratios of  $I_{ij}$  (peak area):

- $L_{ij}$  depends on electronic shell (ex. 1s or 2p); obtained from tables; cancels if taking a peak ratio from same orbitals, ex.  $I_{C_{1s}} / I_{O_{1s}}$
- $C_{inst}$  and  $T(E_{kin})$  are known for most instruments; cancel if taking a peak ratio with  $E_{kin} \approx$  constant, ex.  $I_{C_{1s}(C-C-O)} / I_{C_{1s}(C-CH_3)}$
- $\sigma_{ij}$  obtained from tables; cancels if taking a peak ratio from same atom in different bonding config., ex.  $I_{C_{1s}(C-C-O)} / I_{C_{1s}(C-CH_3)}$
- $\lambda_e$  values can be measured or estimated from empirically-derived expressions

For polymers:  $\lambda_e (nm) = \rho^{-1} (49E_{kin}^{-2} + 0.11E_{kin}^{0.5})$

For elements:  $\lambda_e (nm) = a [538E_{kin}^{-2} + 0.41(E_{kin} a)^{0.5}]$

For inorganic compounds (ex. oxides):

$$\lambda_e (nm) = a [2170E_{kin}^{-2} + 0.72(E_{kin} a)^{0.5}]$$

where:

$$a = \text{monolayer thickness (nm)} \quad a = 10^7 \left( \frac{MW}{\rho N_{Av}} \right)^{1/3}$$

MW = molar mass (g/mol)

$\rho$  = density (g/cm<sup>3</sup>)

$E_{kin}$  = electron kinetic energy (eV)

Ex:  $\lambda_e$  for C<sub>1s</sub> using a Mg K <sub>$\alpha$</sub>  x-ray source:

$$E_B = h\nu - E_{kin}$$

For Mg K <sub>$\alpha$</sub>  x-rays:  $h\nu = 1254 \text{ eV}$

For C<sub>1s</sub>:  $E_B = 284 \text{ eV}$

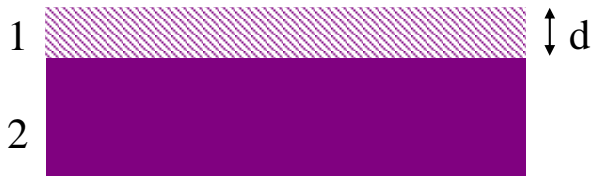
$$\longrightarrow E_{kin} = 970 \text{ eV}$$

$$\lambda_e (nm) = \rho^{-1} \left( 49 E_{kin}^{-2} + 0.11 E_{kin}^{0.5} \right) \quad \text{Assume } \rho = 1.1 \text{ g/cm}^3$$

$$\lambda_e = 3.1 \text{ nm}$$

For non-uniform samples, signal intensity must be deconvoluted to obtain a quantitative analysis of concentration vs. depth.

Case Example: a sample comprising two layers (layer 2 semi-infinite):



$$I_{ij} = C_{ins} T(\text{kin}) L_{ij} \sigma_{ij} \int n_i(z) \exp\left(\frac{-z}{\lambda_e \sin \theta}\right) dz$$

$$I_{ij} = -I_{ij,o}^{(1)} n_{i,1} \lambda_e \sin \theta \exp\left(\frac{-z}{\lambda_e \sin \theta}\right) \Big|_0^d - I_{ij,o}^{(2)} n_{i,2} \lambda_e \sin \theta \exp\left(\frac{-z}{\lambda_e \sin \theta}\right) \Big|_d^{\infty}$$

$$I_{ij} = I_{ij,o}^{(1)} n_{i,1} \lambda_{e,1} \sin \theta \left(1 - \exp\left(\frac{-d}{\lambda_{e,1} \sin \theta}\right)\right) + I_{ij,o}^{(2)} n_{i,2} \lambda_{e,2} \sin \theta \exp\left(\frac{-d}{\lambda_{e,1} \sin \theta}\right)$$

$$\text{or } I_{ij} = I_{ij,\infty}^{(1)} \left(1 - \exp\left(\frac{-d}{\lambda_{e,1} \sin \theta}\right)\right) + I_{ij,\infty}^{(2)} \exp\left(\frac{-d}{\lambda_{e,1} \sin \theta}\right)$$

Why  $\lambda_{e,1}$ ? Electrons originating in semi-infinite layer 2 are attenuated by overlayer 1

where  $I_{ij,\infty}^{(i)}$  = measured peak area from a uniform, semi-infinite sample of material  $i$ .

## Methods to solve for $d$

Scenario 1:  $n_{i,2}=0$  (ex.,  $C_{1s}$  peak of a polymer adsorbed on an oxide):

$$I_{ij} = I_{ij,\infty}^{(1)} \left( 1 - \exp\left(\frac{-d}{\lambda_{e,1} \sin \theta}\right) \right)$$


➤ measure a bulk sample of the upper layer material  $\Rightarrow I_{ij,\infty}^{(1)}$

$$\ln\left(1 - \frac{I_{ij}}{I_{ij,\infty}^{(1)}}\right) = \frac{-d}{\lambda_{e,1} \sin \theta}$$

➤ obtain slope of  $\ln\left(1 - \frac{I_{ij}}{I_{ij,\infty}^{(1)}}\right)$  vs.  $\csc \theta \Rightarrow -d/\lambda_{e,1}$

➤ for a fixed  $\theta$ :

$$d = -\lambda_{e,1} \sin \theta \ln\left[1 - \frac{I_{ij}}{I_{ij,\infty}^{(1)}}\right]$$

➤ substitute a calculated or measured  $\lambda_{e,1}$  to obtain  $d$

Scenario 2:  $n_{i,1}=0$  (ex.,  $M_{2p}$  peak from underlying metal oxide ( $MO_x$ ):

$$I_{ij} = I_{ij,\infty}^{(2)} \exp\left(\frac{-d}{\lambda_{e,1} \sin \theta}\right)$$


➤ measure  $I_{ij}$  for same peak at different take-off angles ( $\theta_1, \theta_2$ )

$$\frac{I_{ij,\theta_1}}{I_{ij,\theta_2}} = \frac{I_{ij,o}^{(2)} n_{i,2} \lambda_{e,2} \sin \theta_1 \exp\left(\frac{-d}{\lambda_{e,1} \sin \theta_1}\right)}{I_{ij,o}^{(2)} n_{i,2} \lambda_{e,2} \sin \theta_2 \exp\left(\frac{-d}{\lambda_{e,1} \sin \theta_2}\right)}$$

$$\frac{I_{ij,\theta_1}}{I_{ij,\theta_2}} = \frac{\sin \theta_1}{\sin \theta_2} \exp\left(\frac{-d}{\lambda_{e,1}} (\csc \theta_1 - \csc \theta_2)\right)$$

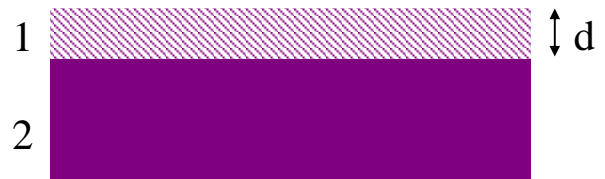
$$d = \lambda_{e,1} (\csc \theta_2 - \csc \theta_1)^{-1} \ln\left(\frac{I_{ij,\theta_1} \sin \theta_2}{I_{ij,\theta_2} \sin \theta_1}\right)$$

➤ substitute a calculated or measured  $\lambda_{e,1}$  to obtain  $d$

Scenario 3: element present in distinguishable bonding configurations in layers 1 & 2 (ex., O<sub>1s</sub> peak from -C-O-C- and MO<sub>x</sub>):

$$I_{ij} = I_{ij,\infty}^{(1)} \left( 1 - \exp\left(\frac{-d}{\lambda_{e,1} \sin \theta}\right) \right) + I_{ij,\infty}^{(2)} \exp\left(\frac{-d}{\lambda_{e,1} \sin \theta}\right)$$

$$\frac{I_{ij}^{(2)}}{I_{ij}^{(1)}} = \frac{I_{ij,o}^{(2)} n_{i,2} \lambda_{e,2} \sin \theta \exp\left(\frac{-d}{\lambda_{e,1} \sin \theta}\right)}{I_{ij,o}^{(1)} n_{i,1} \lambda_{e,1} \sin \theta \left( 1 - \exp\left(\frac{-d}{\lambda_{e,1} \sin \theta}\right) \right)}$$



➤ measure element peak areas  $I_{ij}^{(1)}$  and  $I_{ij}^{(2)}$

➤ for same element and orbital:  $I_{ij,o}^{(1)} = I_{ij,o}^{(2)}$

➤ for same element and orbital:  $\frac{n_{i,2}}{n_{i,1}} = \frac{C_{i,2}}{C_{i,1}}$

$$\frac{I_{ij}^{(2)}}{I_{ij}^{(1)}} = \frac{C_{i,2} \lambda_{e,2} \exp\left(\frac{-d}{\lambda_{e,1} \sin \theta}\right)}{C_{i,1} \lambda_{e,1} \left( 1 - \exp\left(\frac{-d}{\lambda_{e,1} \sin \theta}\right) \right)}$$

➤ solve numerically for  $d$ , substituting calculated values of  $\lambda_{e,2}$  &  $\lambda_{e,1}$

➤ if  $d \ll \lambda_{e,1} \sin \theta$ :

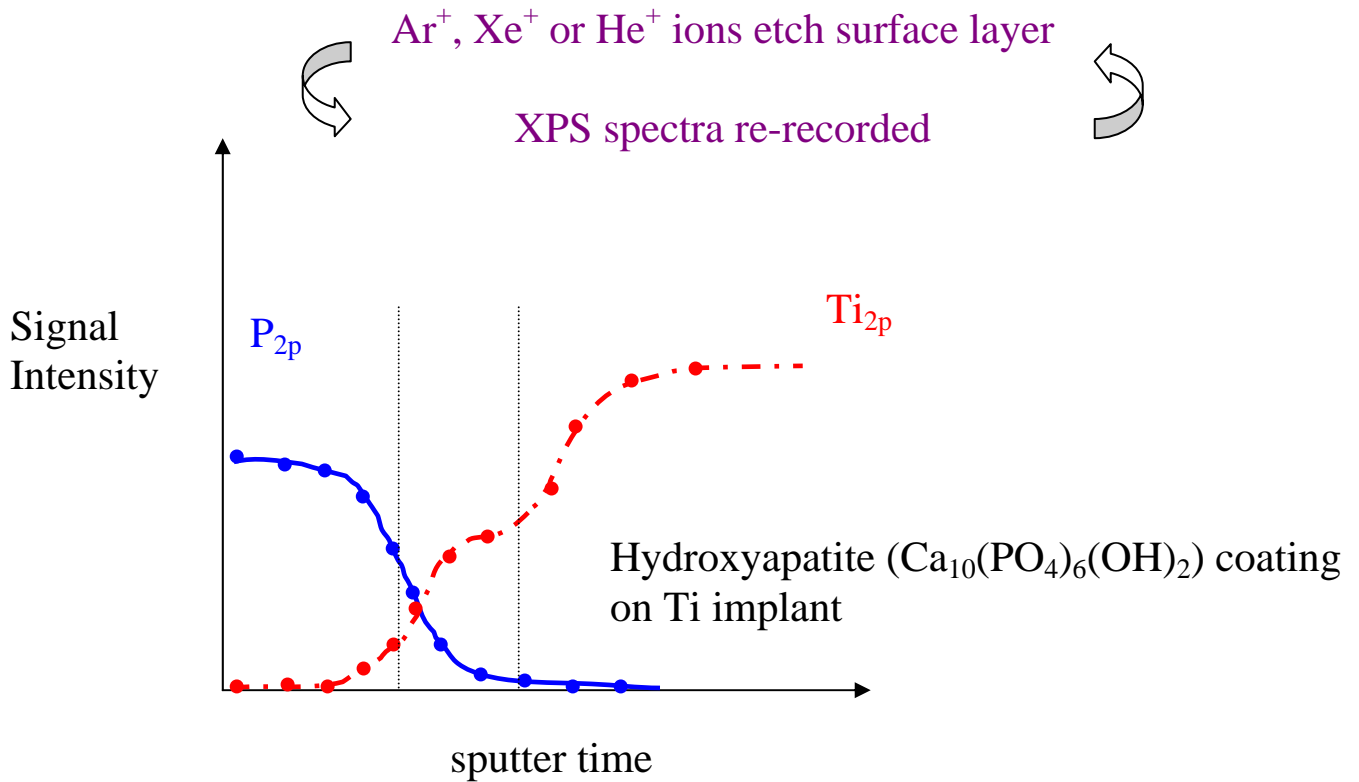
$$\exp(-ax) \approx 1 - ax + \frac{(ax)^2}{2} - \dots$$

$$\frac{I_{ij}^{(2)}}{I_{ij}^{(1)}} = \frac{C_{i,2} \lambda_{e,2} \left( 1 - \frac{d}{\lambda_{e,1} \sin \theta} \right)}{C_{i,1} \lambda_{e,1} \left( \frac{d}{\lambda_{e,1} \sin \theta} \right)}$$

$$d = \lambda_{e,1} \sin \theta \left[ \frac{I_{ij}^{(2)} C_{i,1} \lambda_{e,1}}{I_{ij}^{(1)} C_{i,2} \lambda_{e,2}} + 1 \right]^{-1}$$

## Ion Etching

Depth profiling for depths  $> 10$  nm (100 nm – 1  $\mu$ m)



Calibration of sputter rates: time  $\Rightarrow$  depth

## 2. Auger Electron Spectroscopy

### Theoretical Basis:

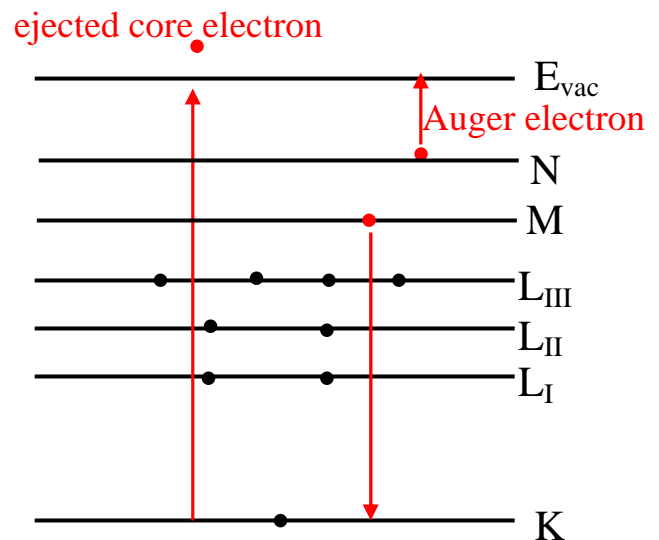
- Auger electrons created by electron bombardment of sample are ejected from near surface (1-3 nm) with characteristic energies
- Analysis of the Auger electron energies yields a quantitative measure of the surface composition

$$E_K - E_M = E_N + E_{\text{kin}}$$

$$E_{\text{kin}} = E_K - E_M - E_N$$

$$E_{\text{xyz}} \text{ (} E_{\text{CVV}} \text{ or } E_{\text{CCV}} \text{)}$$

- ejection from x shell
- electronic transition  $y \rightarrow x$
- release of z-level Auger with  $E_{\text{kin}}$



INFORMATION:  $E_{\text{xyz}}$  is characteristic to element & bonding

### AES vs. XPS

#### Advantages

- focused e-beam gives high x,y spatial resolution (5 nm vs. ~1 μm)
- larger bonding effects

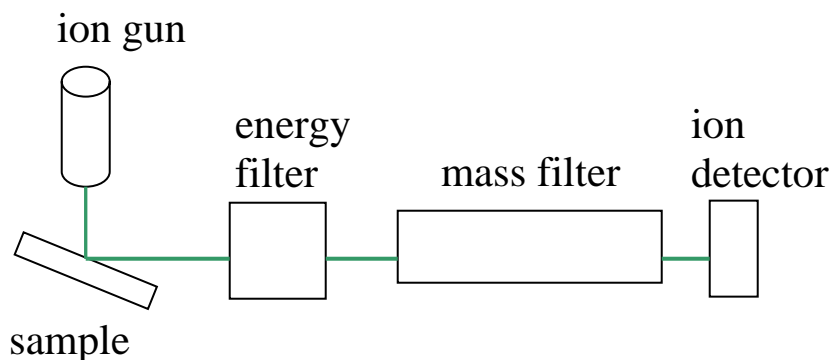
#### Disadvantages

- charging effects on nonconductive samples (unsuitable)
- degradation of organics

### 3. Secondary Ion Mass Spectroscopy (SIMS)

#### Experimental Approach:

- Energetic ions (1-15 keV) bombard sample surface
- Secondary ions/charged fragments are ejected from surface and detected



#### Ion Guns

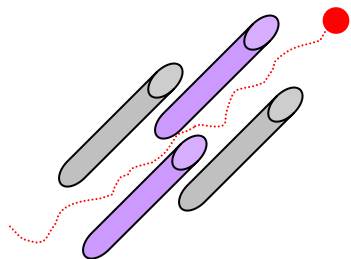
- types {
- Nobel gas:  $\text{Ar}^+$ ,  $\text{Xe}^+$
  - liquid metal ion:  $\text{Ga}^+$ ,  $\text{Cs}^+$  ( $\sim 1\text{nm}$  beam size  $\Rightarrow$  x,y mapping)
  - pulsed LMI (time-of-flight source)
  - low currents used:  $10^{-8}$ - $10^{-11}$  A/cm<sup>2</sup>

Ion beam current (A/cm <sup>2</sup> )	surface monolayer lifetime (s)
$10^{-5}$	16
$10^{-7}$	1600
$10^{-9}$	$1.6 \times 10^5$
$10^{-11}$	$1.6 \times 10^7$

1 Amp =  $6.2 \times 10^{18}$  ions/sec

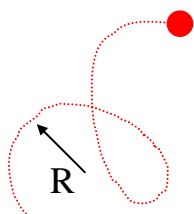
## Detectors

- sensitive to the ratio of mass/charge ( $m/z$ )
- resolution defined as  $m/\Delta m$  (larger = better!)
- Quadrupole (RF-DC): resol.  $m/\Delta m \sim 2000$ ; detects  $m < 10^3$  amu



Oscillating RF field destabilizes ions: only ions with specified  $m/z$  can pass

- Magnetic sector:  $m > 10^4$  amu;  $m/\Delta m \sim 10,000$



Applied B-field results in circular trajectory (radius= $R$ ) of charged particles

$$R = \frac{1}{B} \left( \frac{2mV}{z} \right)^{1/2}$$

accelerating voltage

- Time-of-flight (TOF):  $m \sim 10^3$ - $10^4$  amu;  $m/\Delta m \sim 10,000$

$$time = \left( \frac{m}{2zV} \right)^{1/2} L$$

flight tube length

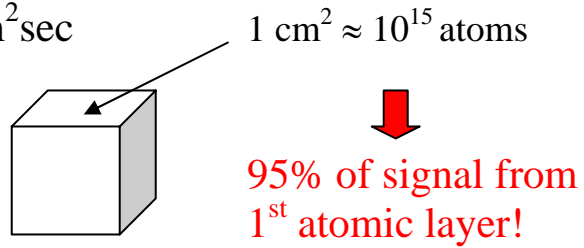
Pulsed primary beam generates secondary ion pulses detected at distance  $L$

## Modes of Operation

### Static SIMS

➤ low energy ions: 1-2 keV; penetration  $\sim 5-10 \text{ \AA}$

➤ low ion doses:  $< 10^{13} \text{ ions/cm}^2\text{sec}$

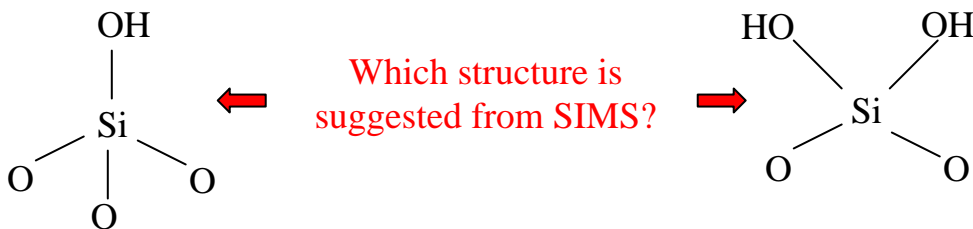
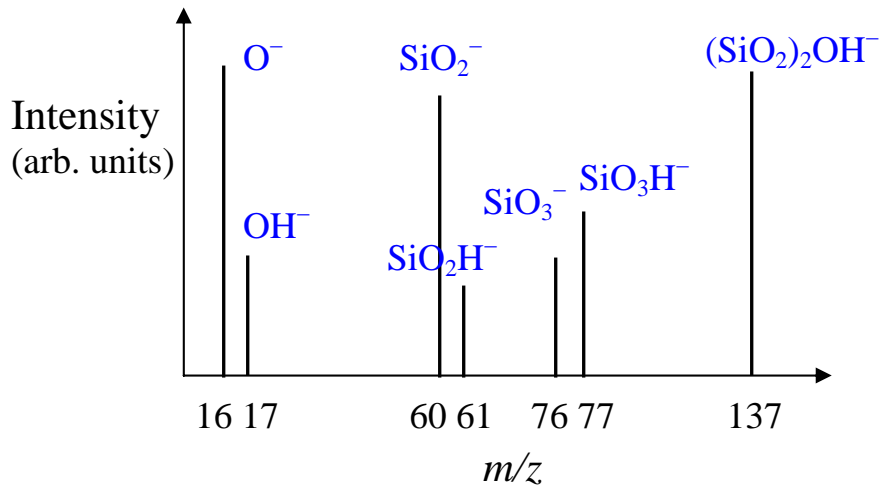


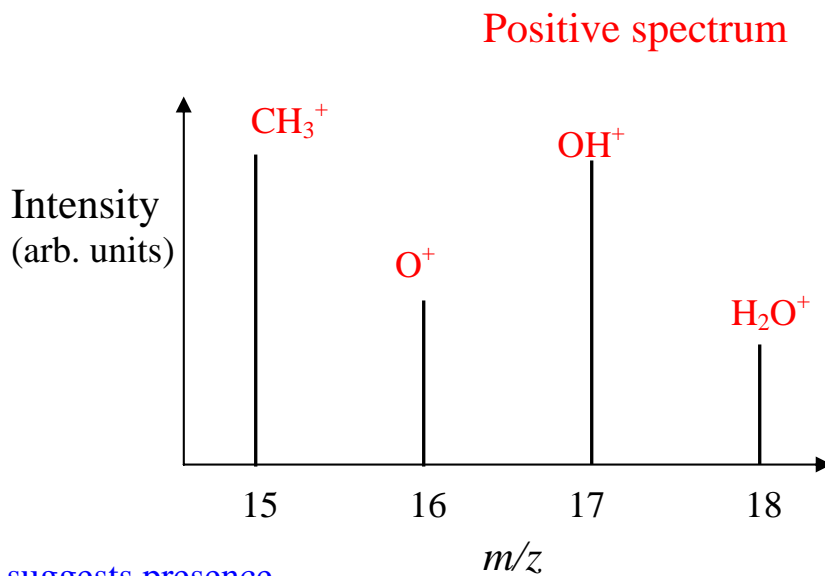
### Information:

- surface composition
- surface bonding chemistry (sputtered fragments)

### Example: SIMS of silica powder

#### Negative spectrum





SIMS suggests presence  
of adsorbed methanol

### SIMS vs. XPS/AES

#### Advantages

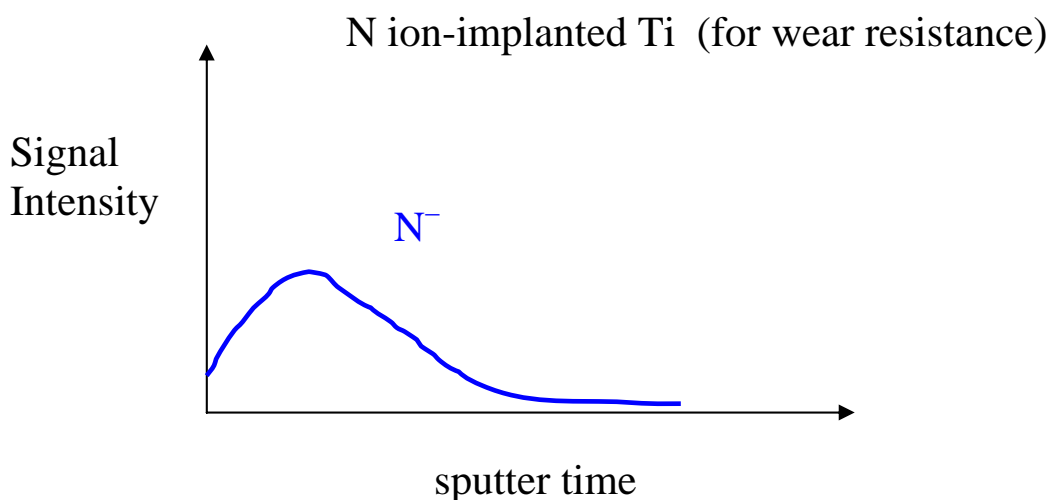
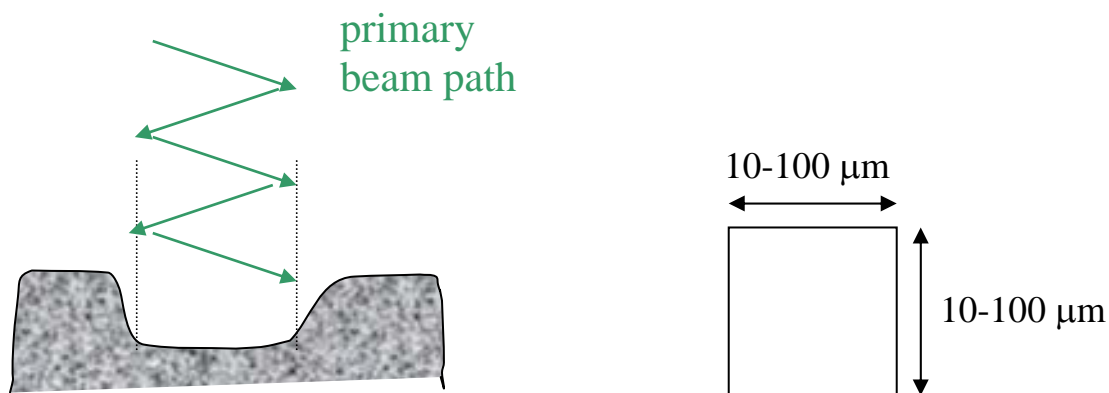
- high sensitivity (ppm – ppb)
- more sensitive to top surface
- applicable to any solid

#### Disadvantages

- not quantitative

### Dynamic SIMS

- 1-20 keV primary beam
- rastered beam sputters a crater in sample
- secondary ions gives depth profiling



### References

J.C. Vickerman, Ed., *Surface Analysis—The Principle Techniques*, J. Wiley & Sons: New York, NY, 1997, Chapters 3, 4 & 5.

D. Briggs, *Surface Analysis of Polymers by XPS and Static SIMS*, Cambridge University Press: United Kingdom, 1998.

C.-M. Chan, *Polymer Surface Modification and Characterization*, Hanson: Cincinnati, OH: 1994, Chapters 3 & 4.

P.J. Cumpson, "Angle-resolved XPS and AES: depth-resolution limits and a general comparison of properties of depth-profile reconstruction methods", *J. Electron Spectroscopy* **73** (1995) 25-52.

B. Elsener and A. Rossi, "XPS investigation of passive films on amorphous Fe-Cr alloys", *Electrochimica Acta* **37** (1992) 2269-2276.

A.M. Belu, D.J. Graham and D.G. Castner, "Time-of-flight secondary ion mass spectroscopy: techniques and applications for the characterization of biomaterial surfaces", *Biomaterials* **24**, (2003) 3635-3653.